IEEE Robotics and Automation Letters (RAL) paper presented at
2024 IEEE/RSJ International Conference on Intelligent Robots and Systems (IROS)
October 14-18, 2024. Abu Dhabi, UAE

CCTV-Informed Human-Aware Robot Navigation in Crowded Indoor Environments

Mincheul Kim[1], Youngsun Kwon[2], Sebin Lee[1], and Sung-eui Yoon[1]

***Abstract*—Mobile robot navigation in crowded indoor environments is a challenging task due to the limited sensing capabilities of onboard sensors. In this study, we propose a mobile robot navigation framework that utilizes external CCTV data to address the limitations of local sensors in a crowded environment. This approach enables mobile robots to navigate safely and efficiently in complex environments by encapsulating human movements from CCTVs to anticipate the human impact on the unclear navigational trajectory of our robot and devise human-aware paths that mitigate collision risks and minimize social intrusions. Further, we integrate a deep reinforcement learning (DRL) algorithm into a generated global path to fine-tune robotic navigation in human-populated areas, enabling the robot to learn efficiently and socially acceptable navigation compared to methods based solely on local sensors. Our experiments further validate the efficiency of using CCTVs to supplement robots with constrained sensing across varied sensor capabilities and CCTVs configurations.**

***Index Terms*—Human-Aware Motion Planning, Task and Motion Planning**

I. Introduction

SERVICE robots are increasingly common in crowded indoor environments such as airports, department stores, and metro stations. However, navigating these environments is challenging due to their large scale, dynamic conditions, and the unpredictable behavior of humans [1] [2]. The robot's onboard sensors, such as LiDAR and RGB-D cameras, further complicate the issue, as they offer only localized, limited-range information, often missing obstacles outside their field of view (FOV) or cannot detect obstacles behind the objects or around corners.

While recent studies have tackled various challenges in robot navigation, including exploration [3], limited FOV [4], and uncertainty [5], most of these solutions rely solely on onboard sensors, inheriting their limitations. A more promising avenue is using external data sources like closed-circuit television (CCTV) cameras, commonly found in the environments where service robots operate. CCTVs are cost-effective, low-maintenance, and strategically placed, offering real-time visual data to enhance a robot's situational awareness. For example, the robot can avoid exploring areas with unknown dangers or densely populated areas in advance by accessing CCTVs information.

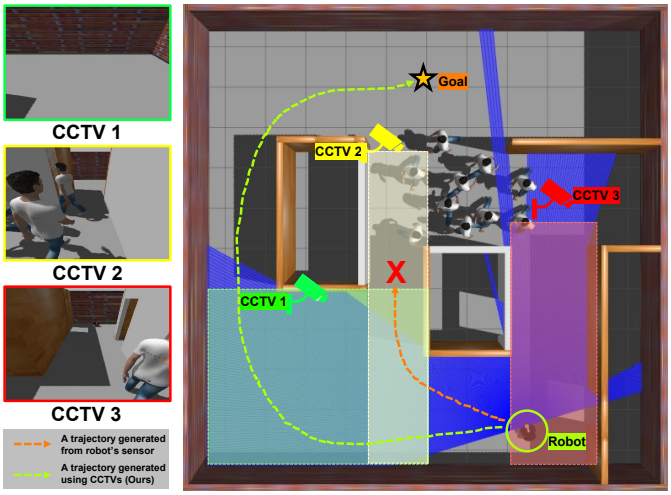

Fig. 1. In this illustration, we demonstrate our navigation framework that complements a robot's local sensing (indicated by the blue area) with data from external CCTVs (shown in different colors). By processing human movements from the CCTVs, our CCTV-informed planner generates human-aware global paths (represented by the green dashed line) in complex and crowded environments. This integrated approach allows the robot to navigate efficiently and safely around dense crowds and potential obstacles.

Previous studies, including Silva *et al.* [6], have focused on predicting human movements using external cameras but have not explored integrating these predictions with robotic navigation strategies. Our framework fills this gap by encapsulating human movements from CCTVs to anticipate human impact on the unclear navigational trajectory of our robot and devise human-aware paths that mitigate collision risks and minimize social intrusions. Further, we incorporate a deep reinforcement learning (DRL) algorithm into our human-aware global path to fine-tune robot navigation in human-populated areas, enabling the robot to learn efficiently and socially acceptable navigation compared to methods based solely on local sensors (see Fig.1).

The contributions of this study are as follows:

1) We present a unique navigation framework that uses external CCTV data to enhance robotic navigation in crowded and dynamic indoor environments.

2) We propose a CCTV-informed global planner that utilizes human detected movements in CCTVs to overcome onboard

Manuscript received: November, 17, 2023; Revised March, 1, 2024; Accepted April, 7, 2024.

This paper was recommended for publication by Editor Aniket Bera upon evaluation of the Associate Editor and Reviewers' comments. This work was supported by IITP and NRF grants funded by the Korea government (MSIT) (RS-2023-00237965(2024) and RS-2023-00208506(2024)). *(Corresponding author: Sung-eui Yoon)*

[1]Mincheul Kim, Sebin Lee, and Sung-Eui Yoon are with School of Computing, Korea Advanced Institute of Science and Technology, Daejeon, South Korea minchkim@kaist.ac.kr, seb.lee@kaist.ac.kr, sungeui@kaist.edu

[3]Youngsun Kwon is with Electronics and Telecommunications Research Institute, Daejeon, South Korea youngsun.kwon@etri.re.kr

Digital Object Identifier (DOI): see top of this page.

sensor limitations and create a comprehensive environmental view facilitating the generation of human-aware global paths.

3) We integrate a deep reinforcement learning network onto a generated global path to learn efficiently and socially acceptable navigation policy.

II. Related Work

A. Robot navigation in a crowds

Many studies investigate mobile robot navigation challenges in crowded indoor settings. A common approach utilizes hand-crafted rules modeling assumed human behaviors, like reciprocal velocity [7] or social force [8]. However, these rules can yield short-sighted paths or freezing robot actions in dynamic environments and easily fall into local optima in complex spaces like long hallways. To address the limitations of traditional algorithms, deep reinforcement learning (DRL) for navigation has gained much attention. Chen *et al.* [9] proposed DRL-based crowd navigation with an attention mechanism. Everett *et al.* [10] handled variable humans via LSTM. Liu *et al.* [11] used a structural-RNN to model robot-human interactions. However, DRL-based navigation tends to be myopic, requires tedious training, and depends on the training environment [12]. Further, many DRL-based methods still rely solely on local sensor inputs, thus remaining unaware of the surroundings beyond their detection range, unable to take proactive risk-averse actions. In contrast, we propose a novel approach leveraging external CCTVs to provide comprehensive spatial awareness derived from CCTVs, allowing for predictive path planning and efficient movement in crowded indoor spaces.

B. Hierarchical path planning

Hierarchical planners are researched for long-term navigation given spatial constraints in indoor environments. They combine a global planner generating paths based on prior spatial knowledge using search methods like A* [13] or RRT [14] and a local planner that follows the path while avoiding observed obstacles. Kastner *et al.* [15] proposed an intermediate planner connecting the global and DRL navigation planners via a waypoint generator. [16] used reinforcement learning to follow global path waypoints for navigation around people. However, previous works assumed that the environment is fully known in advance or that planners immediately reflect environmental changes, which is invalid in crowded indoor settings. To address these issues, we propose a global planner utilizing sparse CCTV data to generate adaptable global paths integrated with a DRL-based local planner, enabling dynamic updates to the global understanding of the environment and leading to more adaptive path planning.

C. Using CCTVs for robot navigation

Recently, video surveillance systems like CCTVs have been applied to tasks like person re-identification, crowd detection, abnormality identification, and event detection. The study [17] detects groups violating social distancing via CCTVs and dispatches a robot to warn them. [6] predicted future motion flows from temporal CCTV data. Ravankar *et al.* [18] solve deadlock situations in crowded alleys using CCTV observations and graph-based priority queue allocation. Related work [19] proposed vision-based localization and path planning using external surveillance cameras indoors. However, it focused on austere environments without considering dynamic obstacles like crowds. In contrast, we propose a navigation framework that integrates CCTV data with human movement analytics to enable human-aware robot navigation even in crowded environments.

III. Methodology

We propose a framework enabling mobile robots to efficiently and safely navigate crowded indoor environments by integrating external CCTV data to overcome the limitations of onboard sensors. First, we describe a CCTV-informed global planner that models the individual space of humans observed from CCTV data, and generate human-aware global paths by incorporating social cost consideration (Sec. III-A). Next, we explain our deep reinforcement learning-based local planner incorporating the global path (Sec. III-B). Fig. 2 provides an overview of the framework.

A. CCTV-Informed global planner

This component generates a human-aware global robot path by incorporating prior static obstacle map data and observed human data from CCTVs into a path planning algorithm. It considers the modeled individual spaces and estimated social costs of observed human to produce collision-free, socially acceptable paths.

Human identification from CCTVs Within the framework of our CCTV-informed global planner, the initial step involves the integration of human detection from CCTVs. We identify humans within CCTV images by utilizing the YOLO [20], assigning unique IDs and calculating their positions and velocities. This process serves as a preliminary stage, aiding in the translation of observed 3D human movements into 2D map locations through homography transformation [21].

Fused map representation. We define a fused cost map, m_{FC}, for the CCTV-Informed global path planning, constructed by aggregating the global occupancy map, m_{GO}, and the individual space map, m_{IS}, representing the detected humans.

The global occupancy map, m_{GO}, is a fixed-resolution grid map encoding static environment structure and obstacles. We assume the robot is already given information about the current environment, such as the global structure and static obstacles. The individual space map, m_{IS}, contains occupied spaces modeled from the observed human movements. Previous studies have represented people as predetermined shapes like circles [22] or grid cells [23]. However, these simplistic representations are inadequate for capturing humans' complex behaviors and intentions, degrading robot navigation performance. To enable better navigation, we model dynamic individual spaces analyzable for path planning by examining observed human movement.

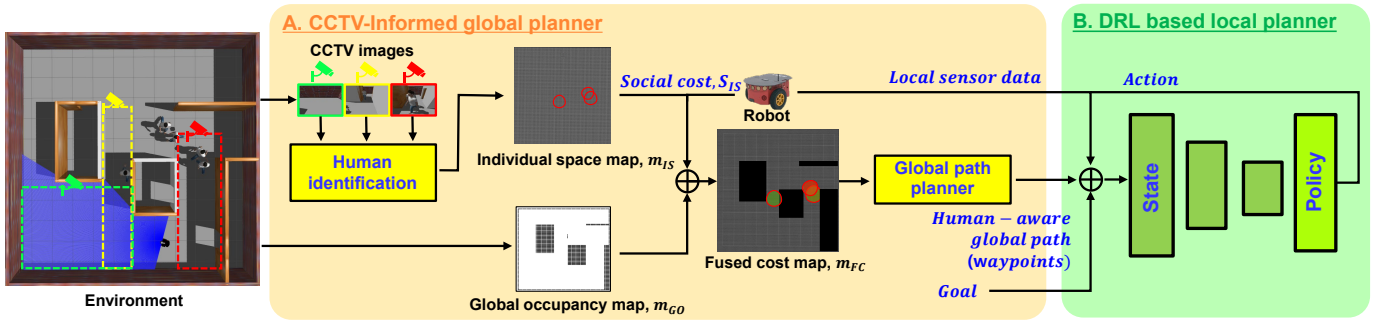

Fig. 2. We propose a hierarchical path planning framework that leverages information from external CCTVs to compensate for the limited local sensor view of robots. The CCTV-informed global planner models individual spaces based on the movements of humans identified from CCTVs and combines this with the prior global occupancy map. It then generates a human-aware global path based on a fused cost map that incorporates social costs reflecting the impact of human movements on the robot. The DRL-based local planner uses the global path as a guide to learn a navigation policy that efficiently and safely reaches the goal.

The individual space model is illustrated in Fig. 3(a). Each human i in the scene is defined by a position $h_i = (x_i, y_i)$, a velocity v_i, and an orientation θ_i. To quantify the area occupied by each human referred to as the individual space IS_i, we adopt the personal space model [24] [25] as a 2D asymmetric Gaussian distribution. Specifically, $IS_i(x, y)$ is given by an exponential function of the form as

$$IS_i(x,y) = e^{-(A(x-x_i)^2+2B(x-x_i)(y-y_i)+C(y-y_i)^2)}, \quad (1)$$

where A, B, and C serve as the coefficients that regulate the geometric configuration of the individual space and are defined as

$$\begin{aligned} A(\theta_i) &= \frac{\cos^2(\theta_i)}{2\sigma^2} + \frac{\sin^2(\theta_i)}{2\sigma_s^2}, \\ B(\theta_i) &= \frac{\sin(2\theta_i)}{4\sigma^2} - \frac{\sin(2\theta_i)}{4\sigma_s^2}, \\ C(\theta_i) &= \frac{\sin^2(\theta_i)}{2\sigma^2} + \frac{\cos^2(\theta_i)}{2\sigma_s^2}. \end{aligned} \quad (2)$$

The value of σ is determined by the facing orientation θ_i and can assume one of two variances: the front variance σ_h or the rear variance σ_r. The respective values for σ_h, σ_s, and σ_r are defined as $\sigma_h = \max(2v_i, 0.5)$, $\sigma_s = \frac{2}{3}\sigma_h$, and $\sigma_r = \frac{1}{2}\sigma_h$.

Finally, the individual spaces for all observed humans are collectively represented in an individual space map m_{IS}, as depicted in Fig. 3(c).

Global path planner with social cost This component produces a human-aware global path that is both collision-free and socially acceptable. It leverages precomputed individual spaces obtained from CCTVs information and incorporates a social cost function into the path planning process.

We propose using a variant of A* algorithm [13] with a new cost function as follows:

$$F(n) = G(n) + H(n) + S_{IS}(n), \quad (3)$$

where n represents a grid cell in the fused cost map m_{FC}. $G(n)$ is the cost from the start point to n, $H(n)$ is a heuristic function that is a conservative approximation of the remaining cost to the goal (e.g., the Euclidean distance), and $S_{IS}(n)$ denotes our newly-introduced social cost function.

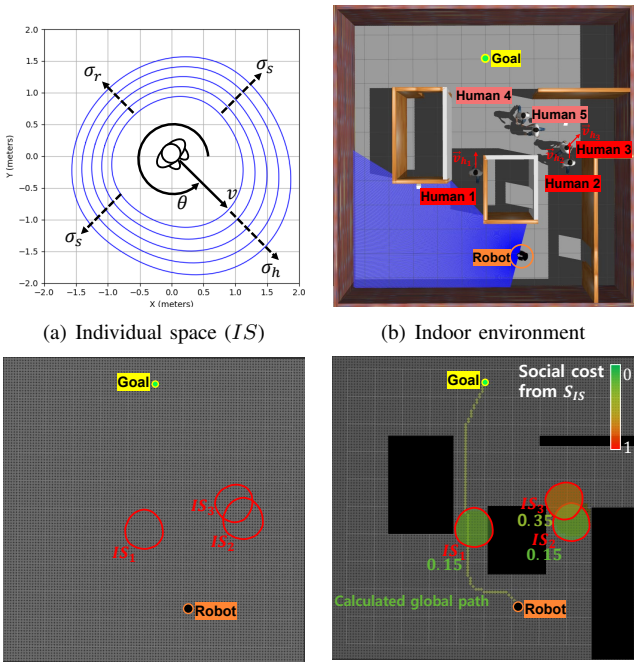

(a) Individual space (IS) (b) Indoor environment

(c) Individual space map (m_{IS}) (d) Human-aware global path

Fig. 3. These figures demonstrate the key elements of the CCTV-Informed global planner. (a) displaces an individual space (IS) centered at (0, 0) with orientation $\theta = 235°$ and velocity $v = 3m/s$. (b) depicts an indoor environment with a robot and moving humans. The robot's sensing range is in semi-transparent blue. People on CCTV and their movements are labeled in red. (c) shows an individual space map m_{IS} integrating all ISs, enclosed by red curves. (d) shows calculated human-aware global path (green dots) by our CCTV-Informed global planner using a fused cost map m_{FC}. Regions in m_{IS} assigned social costs from S_{IS} (numbers below IS labels).

The social cost function, S_{IS}, quantifies the impact of human movement on the robot's path-planning decisions. For this, we introduce a metric called the Intention Alignment Score (τ_j):

$$\tau_j = \frac{\vec{v}_{r\to g} \cdot \vec{v}_{r\to h_j}}{|\vec{v}_{r\to g}||\vec{v}_{r\to h_j}|}, \quad (4)$$

where $\vec{v}_{r\to g}$ represents the robot's "intention" , defined as a goal-oriented vector from its current position towards its goal. $\vec{v}_{r\to h_j}$ refers to the relative velocity vector of the j-th human

compared to the robot. The higher the τ_j, the more closely the $\vec{v}_{r\to h_j}$ aligns with the robot's intention $\vec{v}_{r\to g}$. A high τ_j implies that the robot is more likely to avoid collisions and other negative interactions, and humans are more likely to feel comfortable and safe around the robot.

Based on τ_j, we define our social cost function $S_{IS}(n)$:

$$S_{IS}(n) = \begin{cases} \gamma_1(1-\tau_j), & \text{if } n \in IS_j \\ 0, & \text{else,} \end{cases} \tag{5}$$

where γ_1 is a weight factor set to 0.5, and IS_j is the j-th human's individual space in m_{IS}.

Fig. 3(d) shows a human-aware global path where obstacles block the robot's view of its goal and humans. Utilizing CCTV data, the robot obtains the movements of humans 1, 2, and 3. High S_{IS} costs, driven by humans 2 and 3, discourage the right-side corridor path. Instead, the robot selects a path through the central corridor near human 1, as its movement aligns with the robot's intention, yielding a lower S_{IS} cost. This path ensures efficient and safe navigation to the goal.

Our global path planner recalculates its path at fixed intervals (set as every 2 timesteps), efficiently adapting to environmental changes. This ensures both computational efficiency and the selection of socially acceptable paths aligned with human movements.

B. Deep reinforcement learning based local planner

This component uses a deep reinforcement learning network to achieve robust mobile robot navigation. The navigation policy is optimized using a deep reinforcement learning algorithm considering the robot's observation, state, and the human-aware global path planned in Sec. III-A.

Network architecture. Our DRL-based local planner network is shown in Fig. 4. Below is the system architecture with details:

- State space: The state at each discrete timestep t comprises three primary elements. Initially, L_t represents sensor data as a vector of 20 minimum readings from cone-shaped bins aggregating 3D point-cloud sensor inputs. Additionally, the goal state g_t and the robot state r_t include the robot's relative position and orientation toward its goal alongside its current velocities. Lastly, W_t denotes waypoints in polar coordinates, derived from a human-aware global path from Sec. III-A to enhance decision-making under constrained or unclear local sensor conditions.
- Action space: A non-holonomic mobile robot's motion involves linear velocity (v_t) and angular velocity (ω_t), both of which are limited. v_t ranges from 0 to a maximum of v^{max}, while ω_t ranges from w^{min} to w^{max}.
- Training detail: The network is modeled by Soft Actor-Critic (SAC) algorithm [26] and trained for 1×10^8 timesteps using a learning rate of 3×10^{-4}. It incorporates a discount factor (γ) of 0.99, a replay buffer of 1×10^6, and a batch size 512. The target update coefficient (τ) is set to 0.05, automatically tuning the entropy coefficient (α) to balance exploration and exploitation effectively.

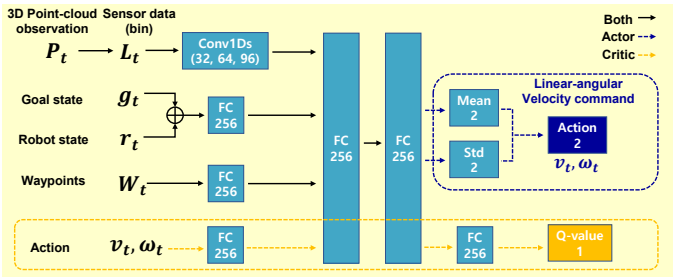

Fig. 4. This figure illustrates a neural network architecture used for deep reinforcement learning (DRL) to develop a navigation policy for a robot. The network takes as input sensor data, a goal state, a robot state, and waypoints from a human-aware global path. It processes these inputs to output an action as linear and angular velocity commands.

Reward function for global guidance. The human-aware global path is critical in compensating for the limited sensors of a robot in order for it to reach its goal in complex and crowded environments. In this context, we introduce a reward function to enhance the robot's ability to navigate towards its goal. This function incorporates waypoints from the global path, aiding the robot's adaptation to environmental changes. We designed the reward function as follows:

$$r^t = R^t_{nav} + R^t_{wpt}, \tag{6}$$

$$R^t_{nav} = \begin{cases} r_g, & \text{if } d^t_{r,g} < \eta_D \\ r_c, & \text{if collision} \\ d^{t-1}_{r,g} - d^t_{r,g}, & \text{otherwise,} \end{cases} \tag{7}$$

where the navigation reward, R_{nav}, is determined as follows: a positive reward r_g is given when the robot's distance to the goal, $d_{r,g}$, is below the threshold η_D set as 0.3 meters. A collision incurs a negative reward r_c. Otherwise, the reward encourages the robot to move closer to the goal. During training, rewards for goal achievement and collision were set at +100 and -100, respectively.

The waypoint reward, R^t_{wpt}, encourages the robot to closely align with the global path, thereby improving navigation performance. First, we identify a subset of waypoints as valid from the waypoint set W_t closer to the goal than the robot's current position. This ensures that the waypoint reward only influences the robot's navigation behavior in a way consistent with its goal. Then, the waypoint reward is determined by measuring the change in distance ($\Delta d_{r,wpt}$) between the robot and each valid waypoint from time $t-1$ to t, formalized as:

$$R^t_{wpt} = \frac{\gamma_2}{N_{wpt}} \sum_{i=1}^{N_{wpt}} \Delta d_{r,wpt_m}, \tag{8}$$

where N_{wpt} is the number of valid waypoints, and $\Delta d_{r,wpt_m} = d^{t-1}_{r,wpt_m} - d^t_{r,wpt_m}$ denotes the change in distance to the $i-$th valid waypoints between consecutive time frames. γ_2 is the weight factor taking a value of 2 if $d^t_{r,wpt_m} > d^{t-1}_{r,wpt_m}$ and 1 otherwise. This weight factor influences the magnitude of the reward and determines whether the robot is attracted to or repelled by each valid waypoint.

IV. EXPERIMENT

A. Implementation detail

To validate our approach, we employed a combination of two simulators: Gazebo [27] and PedSim [28]. The gazebo simulated a 3D indoor environment with strategically positioned CCTVs monitoring extensive areas and high-traffic locations. PedSim simulated crowd behavior, challenging robot navigation with local sensors and emphasizing the need for external sources like CCTVs. Scenarios included detouring congested areas, moving with pedestrian flows, and resembling complex real-world warehouses, detailed in Fig. 5. Our robot, a p3dx-pioneer equipped with a Velodyne-HDL32 LiDAR, captured data over a 180° field with a maximum range of 10m. Each episode randomly assigned start and goal locations, ending upon collision, goal attainment, or after 500 timesteps.

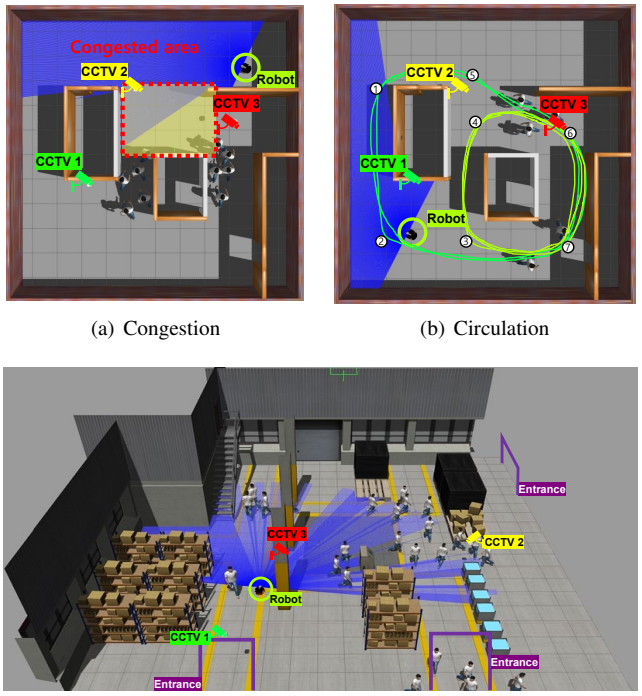

(a) Congestion (b) Circulation

(c) Warehouse

Fig. 5. This figure summarizes the three evaluation scenarios: congestion with people beyond the robot's sensor, circulation with human flows, and a warehouse with diverse human groups and multiple goals.

B. Baselines and evaluation metrics

We compared our model with representative local sensor-based methods for robot navigation, including DWA [29], adapted DRL [3], and the recent socially-aware DRL-VO [30]. Our proposed method is CIGP-DRL (CCTV-informed global planner with deep reinforcement learning), while CIGP-DWA sequentially follows paths generated by CIGP. An ablated model, SimpleGP-DRL, combines DRL with a primary A*-based global planner without considering individual space and social costs.

Evaluation metrics included navigation quality metrics like success rate (SR), average velocity (V_{avg}), and heading change smoothness (ω_{avg}), and social awareness metrics such as intrusion time ratio (ITR) and social distance (SD) used in [31] [32] [33]. All metrics were assessed across 100 episodes to evaluate navigation performance.

TABLE I
NAVIGATION RESULTS IN CONGESTION AND CIRCULATION SCENARIOS SHOW THE **BEST** AND SECOND-BEST PERFORMANCES.

Scenarios	Method	SR(↑)	V_{avg}(↑)	ω_{avg}(↓)	ITR(↓)	SD(↑)
Congestion	DWA [29]	68.0	0.83	0.67	0.16	2.38
	DRL [3]	69.0	0.69	0.47	0.18	2.19
	DRL-VO [30]	73.0	0.77	0.49	**0.13**	2.47
	CIGP-DWA	69.0	0.77	**0.40**	0.15	2.18
	SimpleGP-DRL	75.0	**0.89**	0.56	0.17	2.24
	CIGP-DRL (ours)	**79.0**	0.88	0.46	0.14	**2.74**
Circulation	DWA [29]	39.0	0.68	**0.35**	0.22	1.23
	DRL [3]	68.0	0.78	0.59	0.15	1.61
	DRL-VO [30]	69.0	0.63	0.46	**0.12**	**2.26**
	CIGP-DWA	53.0	0.79	0.46	0.19	1.21
	SimpleGP-DRL	64.0	0.81	0.49	0.18	1.61
	CIGP-DRL (ours)	**74.0**	**0.88**	0.45	**0.12**	2.10

C. Experiment result

Congestion scenario. The quantitative analysis of congestion scenarios presented in Tab. I demonstrates that CIGP-DRL surpasses local sensor-based methods in terms of success rate and achieving faster and smoother movement. This underscores the effectiveness of CCTV-informed global planning for robot navigation. While DRL-VO exhibits superior social awareness performance, CIGP-DRL competes closely, demonstrating its capability to balance navigation efficiency with social considerations. The results highlight the importance of leveraging external CCTVs data to overcome the limitations of local sensor-based navigation approaches.

The qualitative navigation results of the congestion scenario are shown in Fig. 6. DRL struggled in dense crowds, as local sensors failed to detect suddenly appearing humans, leading to collisions due to insufficient reaction time (Fig. 6(a)). SimpleGP-DRL followed its global path without adapting to real-time crowd movements, leading to potential collisions in crowded areas (Fig. 6(b)). DRL-VO aimed to maintain safe distances but frequently opted for longer paths, compromising navigation efficiency with slower speeds (Fig. 6(c)). Our CIGP-DRL, utilizing CCTVs data, navigated around crowds efficiently and safely by adjusting its path in response to real-time congestion, showcasing superior navigation in crowded settings (Fig. 6(d)). This highlights the importance of integrating external data sources for improved navigation in environments where the robot's sensor detection capabilities are limited.

Circulation scenario. Another quantitative navigation results from the circulation scenario are presented in Tab. I. CIGP-DRL achieved the highest navigation performance and demonstrated safety comparable to DRL-VO. This highlights the effectiveness of our CCTV-informed planning approach, which outperforms local sensor-based methods and competes closely with DRL-VO in maintaining safe human distances, enhancing navigation quality and social awareness in dynamic environments.

For example, in Fig. 6(e), DRL struggled to avoid humans behind a central obstacle due to limited sensor range, failing

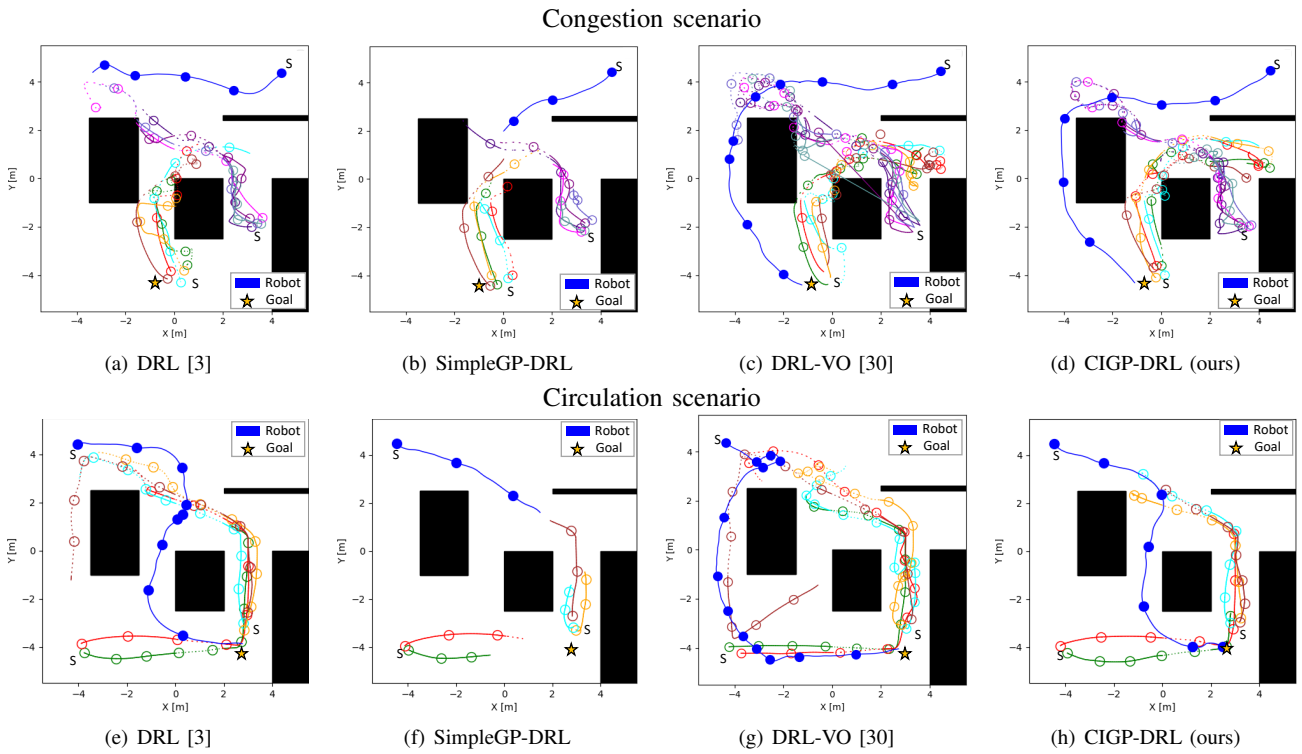

(a) DRL [3] (b) SimpleGP-DRL (c) DRL-VO [30] (d) CIGP-DRL (ours)

(e) DRL [3] (f) SimpleGP-DRL (g) DRL-VO [30] (h) CIGP-DRL (ours)

Fig. 6. Trajectory comparisons of different methods under the experimental scenario. The "S" represents the robot's and the human's starting point, and the star represents the robot's goal. The blue circles show the robot's position at 30-timestep intervals, and the empty circles of different colors show the human's position. The human's trajectory, as seen by the CCTV, is shown as a solid line, and the trajectory of the unseen area is shown as a dotted line. For more details, please see the video.

to predict movements and maintain safe distances, resulting in inefficient navigation. In Fig. 6(f), SimpleGP-DRL collided with humans because its rigid global path did not factor in the movement of people obstructed by the central obstacle. DRL-VO exhibits inefficient navigation performance by overly cautious behavior towards approaching humans, leading to detours and avoidance actions that result in a less efficient path (Fig. 6(g)). In contrast, CIGP-DRL, initially similar to SimpleGP-DRL, proactively adjusts its path based on the social cost calculated from information obtained from CCTV-3, thereby avoiding northward-moving humans. This method underscores the contribution of using external CCTVs data for risk assessment and proactive path optimization, ensuring safe and efficient navigation.

Warehouse scenario. Fig. 5(c) showcases a simulated warehouse designed to reflect real-world complexities, including diverse obstacles and humans. The robot's objective involved navigating multiple subgoals toward a final destination, challenging its adaptability to environmental changes and human interactions. It faced real-world-like scenarios of human-obstructed paths, requiring quick directional adjustments for goal alignment, and necessitated robust navigation amid frequent sensor blockages.

Tab. II demonstrates that our CIGP-DRL significantly outperformed local-sensor based DRL regarding navigation performance and safety. Specifically, Fig. 7(a) and 7(b) compare the responses to scenarios where humans obstructed passage to subgoal 1 without a detour path available. Relying solely on local sensors, DRL struggled with avoiding humans as immediate obstacles but failed to anticipate and evade further humans, leading to collisions. In contrast, at a reduced social cost, CIGP-DRL recalculates a global path through the crowd based on the movement direction of humans blocking the passage. This strategy ensures that the robot navigates in alignment with human movements, thereby facilitating a more efficient path, as depicted in Fig.8(a).

Upon reaching subgoal 2, the robot faced the challenge of significantly adjusting its path to the final goal, as shown in Fig. 7(c) and 7(d). Limited by its dependence on the sensor, DRL struggled to alter its course to avoid collisions, especially with unpredictably moving humans beyond its sensor range. Conversely, CIGP-DRL, leveraging CCTV data for global path planning, enabled smooth path adjustments and avoided potential human approaches, overcoming sensor limitations and ensuring progress toward the final goal.

TABLE II
NAVIGATION RESULTS IN THE WAREHOUSE SCENARIO. THE BEST PERFORMANCE IS DENOTED IN BOLD.

Scenarios	Method	SR(↑)	V_{avg}(↑)	ω_{avg}(↓)	ITR(↓)	SD(↑)
Warehouse	DRL [3]	3.0	0.73	0.80	**0.09**	0.68
	CIGP-DRL (ours)	**33.0**	**0.84**	**0.66**	0.17	**0.77**

D. Evaluating Sensor Compensation and Scalability with CCTV Integration

1) CCTVs compensation for sensor variability: We conducted experiments to assess how our method uses high-level

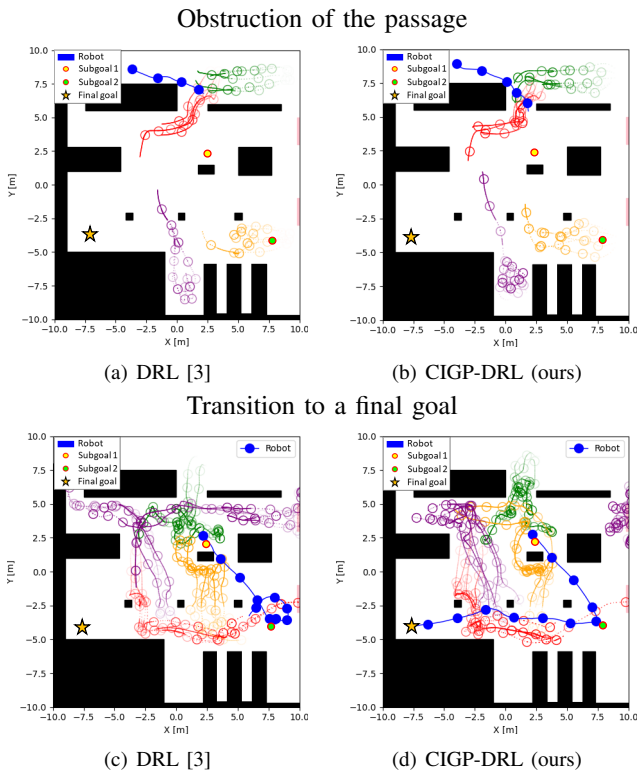

(a) DRL [3] (b) CIGP-DRL (ours)

(c) DRL [3] (d) CIGP-DRL (ours)

Fig. 7. Trajectory evolution comparisons of different methods in challenging situations within the warehouse scenario. As the robot moves towards subgoal 1, its path is blocked by the crowd (Obstruction). Upon reaching subgoal 1, the robot has to navigate through the crowd and make a sharp path transition to pass through subgoal 2 en route to the final goal (Transition).

external information to offset the constraints of local sensors. The evaluation was set in the circular scenario (Fig. 5(b)), focusing on sensor limitations amidst varied human movements. We compared DRL [3], reliant solely on local sensors, against our CIGP-DRL, incorporating a human-aware global path. We varied the robot's sensing range from 10 meters down to 2 meters.

The results are shown in Fig. 9. As the sensor range decreased, DRL's success rate and travel time deteriorated significantly, reflecting the challenges posed by limited data access. However, our CIGP-DRL retained robust performance, confirming its effectiveness in tapping external data to counteract local sensor shortcomings.

2) Scalability with varied CCTVs Inputs: Through the systematic adjustment of CCTV configurations from none to omnipresent coverage in the circulation scenario, this study investigates how varying levels of environmental uncertainty affect our CIGP-DRL framework's performance, marking a transition from complete uncertainty to full environmental awareness.

Findings in Tab. III reveal a significant correlation between increased environmental information from CCTV data and improved navigation performance, highlighting our method's capacity to adaptively reduce navigational uncertainties and enhance efficacy as environmental clarity escalates, thereby demonstrating its robust scalability and effectiveness across varying degrees of environmental uncertainty.

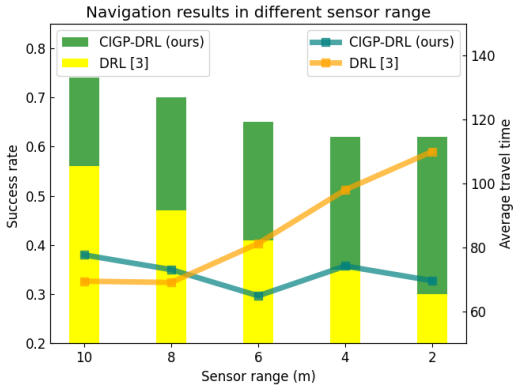

Fig. 9. Evaluation of DRL and CIGP-DRL results according to different robot sensor ranges in the circulation scenario. The bar plot shows the success rate, and the line plot shows the navigation time in case of success. CIGP-DRL, which utilizes a human-aware global path, achieves a higher success rate and lower navigation time than local-sensor based DRL.

TABLE III
NAVIGATION RESULTS WITH DIFFERENT CCTVS SETUP.

Number of CCTVs	**0**	**1**	**2**	**3**	∞
Success rate (SR)	64.0	68.0	70.0	74.0	81.0

V. LIMITATIONS AND FUTURE WORK

This section identifies our study's limitations and future research directions. Key challenges include the diminished effectiveness of our method in dense crowds, such as in busy transit hubs or emergency evacuations, where occlusions and complex group dynamics hinder individual tracking. Our simulations may not fully capture the stochastic nature of human behavior, leading to potentially unrealistic predictions. Future efforts will aim to validate our method using advanced simulations or real-world data, improve global path planning through analysis of group movement patterns [34], and develop risk assessment models for unexplored areas [35] [36]. We will also enhance real-time data processing and develop strategies for optimal CCTV placement to maximize environmental coverage.

VI. CONCLUSION

In this study, we introduce a mobile navigation framework that leverages external CCTV data, addressing the constraints of local sensors in crowded indoor environments. Our CCTV-Informed global planner employs social costs to calculate human-aware global paths that circumvent unseen risks like congestion. This social cost is derived from the individual spaces formed from human movement and the alignment of the robot's intentions with those of humans. A deep reinforcement learning model then incorporates this global path with the robot's state to deduce an optimal navigation policy. Empirically, our approach outperforms predominantly local sensor-dependent methods, both quantitatively and qualitatively. Our experiments further validate the efficiency of using CCTVs

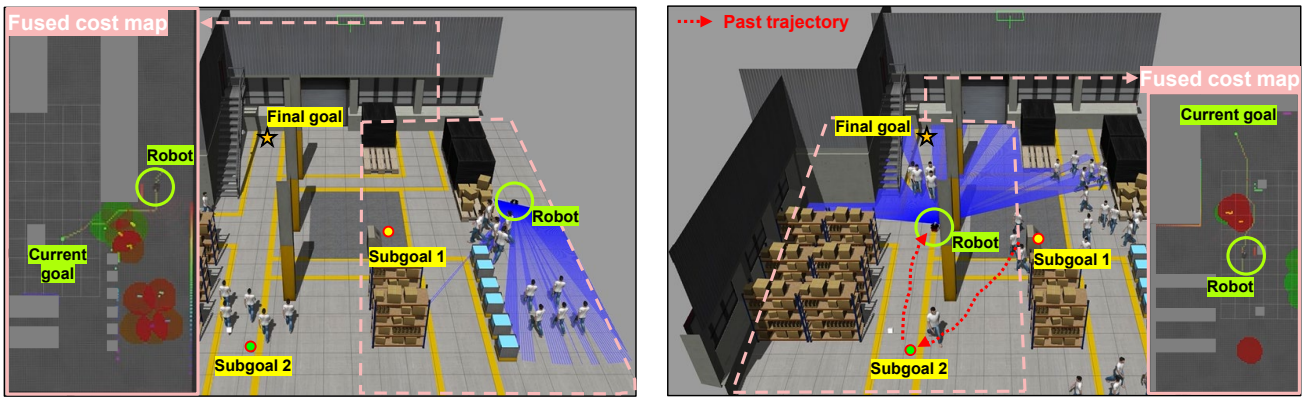

(a) Obstruction of the passage

(b) Transition to a final goal

Fig. 8. Navigation results of CIGP-DRL in a warehouse environment are as follows: (a) despite the pathway to subgoal 1 being obstructed by the crowd, the robot navigates by utilizing a global path that considers the direction of the crowd's movement, obtained from CCTVs, thereby allowing it to follow behind the crowd. (b) from subgoal 2 to the final goal, despite the need for abrupt direction changes, the robot executes smooth transitions using the global path and moves along a preemptive detour path, considering the risk of approaching humans.

to supplement robots with constrained sensing across varied sensor capabilities and CCTV configurations.

Building on the discussions and future work outlined, future research will concentrate on enhancing the navigation strategy with different human behavior modeling and extending the framework's applicability to real-world scenarios.

REFERENCES

[1] T. Kruse, A. K. Pandey, R. Alami, and A. Kirsch, "Human-aware robot navigation: A survey," *Robot. Auton. Syst.*, vol. 61, no. 12, 2013.
[2] A. Vemula, K. Mülling, and J. Oh, "Modeling cooperative navigation in dense human crowds," in *ICRA*. IEEE, 2017.
[3] R. Cimurs, I. H. Suh, and J. H. Lee, "Goal-driven autonomous exploration through deep reinforcement learning," *IEEE Robot. Autom. Lett.*, vol. 7, no. 2, pp. 730–737, 2021.
[4] K. Katyal, K. Popek, C. Paxton, P. Burlina, and G. D. Hager, "Uncertainty-aware occupancy map prediction using generative networks for robot navigation," in *ICRA*. IEEE, 2019.
[5] T. Fan, P. Long, W. Liu, J. Pan, R. Yang, and D. Manocha, "Learning resilient behaviors for navigation under uncertainty," in *ICRA*. IEEE, 2020.
[6] G. Silva, K. Rekik, and A. Kanso, "A step towards human-aware path planning based on a combination of partial motion flows," in *ICRA Workshop on Social Robot Navigation: Advances and Evaluation*. IEEE, 2022.
[7] J. Van den Berg, M. Lin, and D. Manocha, "Reciprocal velocity obstacles for real-time multi-agent navigation," in *ICRA*. IEEE, 2008.
[8] M. Kamezaki, Y. Tsuburaya, T. Kanada, M. Hirayama, and S. Sugano, "Reactive, proactive, and inducible proximal crowd robot navigation method based on inducible social force model," *IEEE Robot. Autom. Lett.*, vol. 7, no. 2, pp. 3922–3929, 2022.
[9] C. Chen, Y. Liu, S. Kreiss, and A. Alahi, "Crowd-robot interaction: Crowd-aware robot navigation with attention-based deep reinforcement learning," in *ICRA*. IEEE, 2019.
[10] M. Everett, Y. F. Chen, and J. P. How, "Motion planning among dynamic, decision-making agents with deep reinforcement learning," in *IROS*. IEEE, 2018.
[11] S. Liu, P. Chang, W. Liang, N. Chakraborty, and K. Driggs-Campbell, "Decentralized structural-rnn for robot crowd navigation with deep reinforcement learning," in *ICRA*. IEEE, 2021.
[12] X. Xiao, B. Liu, G. Warnell, and P. Stone, "Motion planning and control for mobile robot navigation using machine learning: A survey," *Auton. Robots*, vol. 46, no. 5, p. 569–597, jun 2022.
[13] P. Hart, N. Nilsson, and B. Raphael, "A formal basis for the heuristic determination of minimum cost paths," *IEEE Trans. Syst. Man. Cybern.*, vol. 4, no. 2, pp. 100–107, 1968.
[14] S. M. LaValle, "Rapidly-exploring random trees : a new tool for path planning," *The annual research report*, 1998.
[15] L. Kästner *et al.*, "Connecting deep-reinforcement-learning-based obstacle avoidance with conventional global planners using waypoint generators," in *IROS*. IEEE, 2021.
[16] C. Pérez-D'Arpino, C. Liu, P. Goebel, R. Martín-Martín, and S. Savarese, "Robot navigation in constrained pedestrian environments using reinforcement learning," in *ICRA*. IEEE, 2021.
[17] A. J. Sathyamoorthy, U. Patel, M. Paul, Y. Savle, and D. Manocha, "Covid surveillance robot: Monitoring social distancing constraints in indoor scenarios," *Plos one*, vol. 16, no. 12, 2021.
[18] A. Ravankar, A. Ravankar, Y. Kobayashi, and T. Emaru, "Intelligent robot guidance in fixed external camera network for navigation in crowded and narrow passages," in *Proceedings*. MDPI, 2016.
[19] J.-H. Shim and Y.-I. Cho, "A mobile robot localization using external surveillance cameras at indoor," *Procedia Computer Science*, vol. 56, pp. 502–507, 2015.
[20] G. Jocher, "YOLOv5 by Ultralytics," 5 2020. [Online]. Available: https://github.com/ultralytics/yolov5
[21] R. Hartley and A. Zisserman, *Multiple view geometry in computer vision*. Cambridge university press, 2003.
[22] E. T. Hall and E. T. Hall, *The hidden dimension*. Anchor, 1966.
[23] S. Yao, G. Chen, Q. Qiu, J. Ma, X. Chen, and J. Ji, "Crowd-aware robot navigation for pedestrians with multiple collision avoidance strategies via map-based deep reinforcement learning," in *IROS*. IEEE, 2021.
[24] A. Wang and A. Steinfeld, "Group split and merge prediction with 3d convolutional networks," *IEEE Robot. Autom. Lett.*, vol. 5, 2020.
[25] R. Kirby, *Social robot navigation*. Carnegie Mellon University, 2010.
[26] T. Haarnoja, A. Zhou, P. Abbeel, and S. Levine, "Soft actor-critic: Off-policy maximum entropy deep reinforcement learning with a stochastic actor," *CoRR*, vol. abs/1801.01290, 2018.
[27] N. Koenig and A. Howard, "Design and use paradigms for gazebo, an open-source multi-robot simulator," in *IROS*. IEEE, 2004.
[28] "Pedsim_ros," https://github.com/srl-freiburg/pedsim_ros, online; accessed 11-October-2020.
[29] D. Fox, W. Burgard, and S. Thrun, "The dynamic window approach to collision avoidance," *IEEE RA-M*, vol. 4, no. 1, pp. 23–33, 1997.
[30] Z. Xie and P. Dames, "Drl-vo: Learning to navigate through crowded dynamic scenes using velocity obstacles," *IEEE T-RO*, 2023.
[31] S. Liu *et al.*, "Intention aware robot crowd navigation with attention-based interaction graph," in *ICRA*, 2023.
[32] A. Francis *et al.*, "Principles and guidelines for evaluating social robot navigation algorithms," *arXiv preprint arXiv:2306.16740*, 2023.
[33] J. Karwowski and W. Szynkiewicz, "Quantitative metrics for benchmarking human-aware robot navigation," *IEEE Access*, 2023.
[34] M. Kim, Y. Kwon, and S.-E. Yoon, "Group estimation for social robot navigation in crowded environments," in *ICCAS*. IEEE, 2022.
[35] H. Yang, J. Lim, and S.-E. Yoon, "Anytime rrbt for handling uncertainty and dynamic objects," in *IROS*. IEEE, 2016.
[36] K. Johansson, U. Rosolia, W. Ubellacker, A. Singletary, and A. D. Ames, "Mixed observable rrt: Multi-agent mission-planning in partially observable environments," in *ICRA*. IEEE, 2023.